International Journal of Modern Physics B
Vol. 18, No. 15 (2004) 2123–2139

World Scientific
www.worldscientific.com

THE "FOLDING" BEHAVIORS OF HOMOPOLYMERS WITH ONE END FIXED

BIN XUE

National Solid State Microstructure Lab, Institute of Biophysics and Department of Physics, Nanjing University, Nanjing 210093, P. R. China
xuebin@biophy.nju.edu.cn

JUN WANG

National Solid State Microstructure Lab, Institute of Biophysics and Department of Physics, Nanjing University, Nanjing 210093, P. R. China
jwang@biophy.nju.edu.cn

WEI WANG*

National Solid State Microstructure Lab, Institute of Biophysics and Department of Physics, Nanjing University, Nanjing 210093, P. R. China
wangwei@nju.edu.cn

Received 28 June 2003

We study the "folding" behaviors of homopolymers with one end fixed. By using canonical ensemble molecular dynamics simulation method, we observe the conformational changes during folding processes. Long chains collapse to the helical nuclei, then regroup to helix from the free-end to form the compact conformations through the middle stages of helix-like coil and helix-like cone, while short chains do not apparently have the above mentioned middle stages. Through simulated annealing, the native conformation of homopolymer chain in our model is found to be helix. We show the relations between specific heat $C_{\rm v}(T)$ and radius of gyration $R_{\rm g}(T)$ as functions of temperature, chain length and the interaction strength, respectively. We find that these two quantities match well and can be combined to interpret the "folding" process of the homopolymer. It is found that the collapse temperature T_θ and the native-like folding temperature $T_{\rm f}$ do not change with the chain length in our model, however the interaction strength affects the values of T_θ and $T_{\rm f}$.

Keywords: Homopolymer; molecular dynamics; nuclei.

1. Introduction

Protein folding is an interesting and important process in molecular biology. Many models have been proposed to simplify and mimic the folding behavior.[1–10] In

*Correspondence author.

these studies, proteins are treated as heteropolymers with finite length by lattice models,[7,8] or by off-lattice ones.[1−4] Under the off-lattice situation, models varying from all-atom ones to coarse-grained ones have all been studied using Monte Carlo method (MC) and Molecular Dynamics simulation (MD). The thermodynamic and dynamic properties, as well as various microscopic folding mechanisms are investigated.[1−13] The basic features of protein chain, such as the topology, the excluded volume and the hydrophobicity, are considered as the starting points of the folding studies.

The complicated folding behaviors also attribute to the complex environment. The crowded surroundings, and specific agents (such as chaperone) may greatly affect the folding process. Even the peripheral membrane protein may alter its folding process since the folding of various parts of protein chain may be initiated differently. These processes are also important for the understanding on the operation of biological machinery. However, the high density and heterogeneity make the modeling of the environment rather difficult.

In this paper, we report a study on the homopolymer model chain with one terminals fixed as a constraint. This simplified model comes from a specific stage of protein synthesis when the chain has some constraints. During the synthesis of the peptide chain in the ribosome, the newly synthesized peptide chain is still connected to ribosome complex. In this stage, the folding behaviors of the peptide segment are physically like that of a chain with one end fixed due to the large mass of the ribosome complex. Although the homogeneity of the chain is not enough to represent the real protein, it is simple and useful to give physical implications to other relevant issues of interest, for example, in the case of adhering and adsorption of macromolecule. The collapse and folding of such a restricted chain may behave differently from a regular "free" chain. What kinds of patterns would the chain prefers to take? How does the folding proceed? These questions may act as a starting point to study more complex situations. For the cases in this paper, various dynamic and thermodynamic properties of the model homopolymer chains with different sizes are studied, especially the folding processes. The nucleation mechanism during the collapse is found to be important for the folding process.[14,15] The long chains take the nucleation mechanism and evolute through specific middle stages while the short chains have no such middle stages obviously. The collapse and "folding" temperatures are affected by the interaction strength linearly.

2. Model and Method

Since the homopolymer under our consideration is relatively flexible with multiple formalities, it is modeled as a chain of monomers with every two consecutive monomers are linked by virtual bond. Each monomer on the homopolymer chain is treated as a bead with a certain radius. The chain length refers to the number of the beads N. The total potential energy is a summation of the bond interaction

and the Van der Waals interactions as

$$U = U_{\text{bond}} + U_{\text{LJ}} \,. \tag{1}$$

The bond interaction is modeled by a quadratic and quartic potential

$$U_{\text{bond}} = \sum_{j=1}^{N-1} k_1 (r_{j,j+1} - d_0)^2 + k_2 (r_{j,j+1} - d_0)^4 \,, \tag{2}$$

where, $r_{j,j+1}$ is the distance between two consecutive beads, $d_0 = 3.8$ Å is the equilibrium distance of the bond, $k_1 = \varepsilon$ and $k_2 = 100\varepsilon$ are the bond interaction strengths with ε being the reduced energy unit.[16] The quadratic term characterizes the consecutive beads as a harmonic oscillator, while the quartic term acts as a "soft clamp" whose function is to restrict the beads not far away from the equilibrium distance d_0. For the interaction between two non-consecutive beads, a 12–6 Leonard–Jones (LJ) potential is used[2,17]

$$U_{\text{LJ}} = \lambda\varepsilon \left[\left(\frac{\sigma_{ij}}{r_{ij}} \right)^{12} - 2 \left(\frac{\sigma_{ij}}{r_{ij}} \right)^{6} \right] . \tag{3}$$

Here λ is the interaction strength, r_{ij} is the distance between the two non-consecutive beads i and j, σ_{ij} is the equilibrium distance between them. For simplicity, all σ_{ij} are set as 6.5 Å. It is noted that the solvent effect is implicitly combined into the above potential Eq. (3). The interaction strength λ may be adjusted to mimic different solvent conditions. Obviously, since the homopolymer chains under our consideration have good flexibility, the potentials do not include the local constraints, which are usually represented by the bond-angle potential and the dihedral potential.[2]

For the cases we are interested in, the homopolymer chain is usually attached to a complex of various molecules, such as ribosome or membrane. The complex system is generally much heavier than our interested homopolymer chain. Consequently, the complex system can be considered as unmovable, and serves as a restriction for the homopolymer chain. Therefore, in our study, the first bead is always fixed at its initial position, whereas the other beads are free to move.

Molecular dynamics (MD) method is used to simulate the folding process of the model chain by numerically solving the Newtonian equations of the beads through direct Eular integration. The integration time step h in the simulation is set to be $h = 0.005\tau$, where $\tau = a\sqrt{m/\varepsilon}$ is the character time of the system with m the mass of one bead. Here, reduced units are used, namely $m = 1$, $\varepsilon = 1$, $a = 1$, and then $\tau = 1$. [Actually, these parameters are related to the real situation if we take $m = 3 \times 10^{-22}$ g, $\varepsilon = 1$ kcal/mol, and $a = 5$ Å. Thus, the character time is about 3×10^{-12} s, and the integration time step is about 15 fs. (see Ref. 1) Berendsen's velocity rescaling is utilized to realize the canonical ensemble in our simulations.[18] The Berendsen coupling coefficient, b, is chosen as $b = 0.0005$.

The initial conformation of the chain is a straight line, the initial velocities are set to satisfy the Maxwell distribution at the given temperature. The regular total

simulation steps are 2×10^7, in which the first 2×10^6 to 4×10^6 steps are used for equilibrating the system, which base on and vary according to the chain length. The samples are taken every 1×10^5 steps. The ensemble average of every physical quantity is calculated by averaging the samples over that trajectory after reaching the equilibrium. And up to 120 runnings are performed at each temperature by setting different initial velocities to get the convergence results.[1]

To characterize the properties of equilibrium state, the following geometrical and thermodynamical quantities are used. One is the radius of gyration R_{g}, defined as,

$$R_{\mathrm{g}} = \left\langle \sqrt{\frac{1}{N} \sum_{i=1}^{i=N} (\mathbf{r}_i - \mathbf{r}_c)^2} \right\rangle , \tag{4}$$

where $\langle \cdots \rangle$ denotes the ensemble average, $\mathbf{r}_i$ is the position vector for bead i, $\mathbf{r}_c$ is the position vector for mass center of the chain. R_{g} measures of the rough size of the chain. Another valuable quantity is the heat capacity,

$$C_{\mathrm{v}} = \frac{\langle E^2 \rangle - \langle E \rangle^2}{T^2} , \tag{5}$$

where E represents the energy in a certain conformation. C_{v} indicates the energy variations of the chain system, which provides more information on the compactness of the chain. We also calculate the position fluctuation for every bead to show its relative motion.

$$\delta r_i^2 = \langle r_i^2 \rangle - \langle r_i \rangle^2 , \tag{6}$$

where δr_i^2 is the position fluctuation of ith bead, $\langle \cdots \rangle$ indicates the average over the trajectory after reaching the equilibrium.

3. Results and Discussion

The evolutions of the total energy E_{T}, namely the sum of kinetic energy E_{K} and potential energy E_{P}, for a chain of $N = 60$ are shown in Fig. 1(a). As can be seen in Fig. 1(a), within a very short time of 3×10^4 to 4×10^4 simulation steps, the values of total energy E_{T} drop quickly to the equilibrium. This means that there is a "folding" tendency which induces the chain into a compact conformation. Under different temperatures, the times for the chain to reach the equilibrium states change slightly. However, the equilibrium values of the total energy are different at different temperatures, indicating different degrees of compactness. Figure 1(b) shows the changes of the radius of gyration R_{g} at different temperatures. Large value of R_{g} refers to large volume of the chain, indicating the chain is loose, and *vice versa*. As shown in Fig. 1(b), the values of R_{g} also drop quickly, similar to that of the total energy. At temperatures of $T = 0.1$, 0.2 $T = 0.4$ and 0.5, the average values of R_{g} are 9.56, 9.21, 9.24 and 9.43, respectively. It is interesting to note that

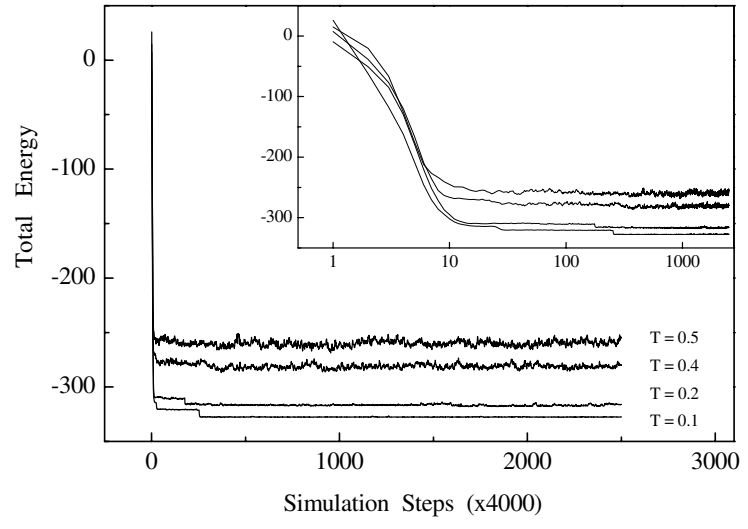

(a)

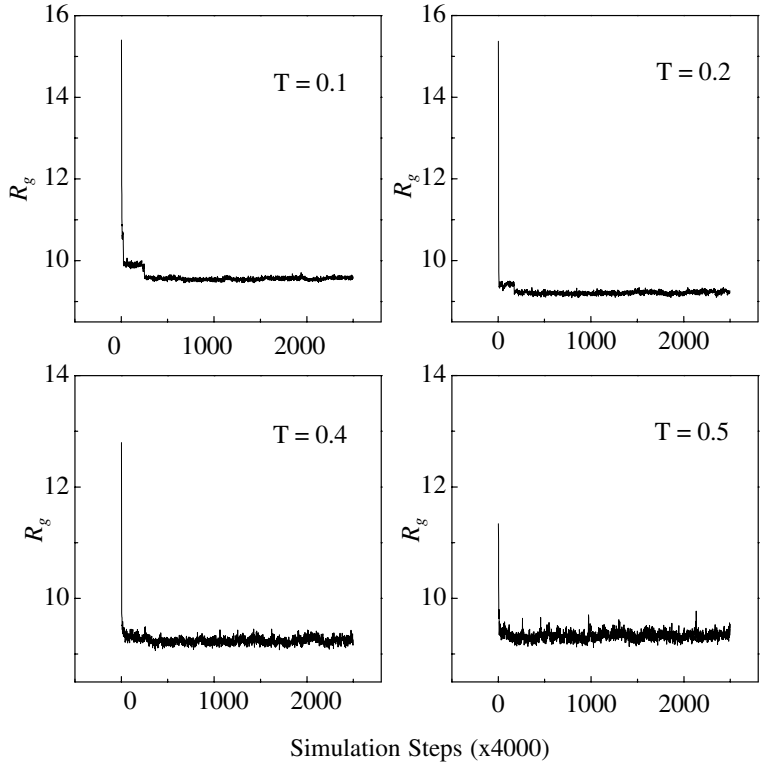

(b)

Fig. 1. The changes of total energy E_{T} and radius of gyration R_{g} during the simulation for chain of $N = 60$ at temperatures of $T = 0.1$, 0.2, 0.4 and 0.5. (a) The evolution of total energy. (b) The evolution of R_{g}. Inset shows the data on a log base.

the minimum value of R_g appears at $T = 0.25$, which is in the middle range of simulation temperatures. As we will show later, in our model the native conformation of the homopolymer chain at low temperature is a helix. While slightly raising the temperature, the native conformation is destructed and the homopolymer chain takes the form of a globule. From the view of energy, raising temperature increases the kinetic energy, and then the potential energy too. However since the increment in temperature is small, the increasing of potential energy is also finite. Hence the distances among beads do not increase prominently. As a result, R_g of the globule at a slightly higher temperature is less than that of the helix at a lower tempearture. This is the reason why the radius of gyration will decrease with slightly increasing the temperature until the temperature is high enough.

Figure 2 shows an example of the folding process of a chain with $N = 60$ at temperature $T = 0.1$. The initial conformation of the chain is a straight line and the fixed end is indicated by the number "1" (see Fig. 2). Under the effect of hydrophobicity, the chain shrinks quickly. This is the collapsing process. Clearly, three nuclei are formed at $t = 1000$ as shown in Fig. 2(a). This conclusion can be confirmed in Fig. 3 too. Here, the nucleus refers to the aggregation of neighboring beads at the early stage of the "folding", and the nucleus has no dimension limitation in the current paper. Then the chain begins to form helices at the positions where the nuclei locate. There are three helix-like coils aligned along the horizontal direction at $t = 10,000$ [see Fig. 2(b)]. The helix-like coils have different numbers of rolls, radii and pitches of screws. The helix-like coil near the free-end forms at the earliest time and has the largest radius of helical spring which is 6.39 Å. The radii for other two smaller helix-like coils are 3.89 Å and 4.34 Å, respectively. The largest coil further starts to merge with other two smaller coils. The three coils are combined together and evolute to a large spring-cone with the fixed end as the apex. The radius of the helical spring at the free-end is 3.83Å, and the values of radii gradually reduce to zero at the fix-end. So, this conformation is a helix-like cone. Such collapse and coil-merging processes are clearly shown in Figs. 2(b) and 2(c). Finally the chain is in a stable state which has the conformation of helix as shown in Fig. 2(c). Further annealing simulation of the same chain confirms that the helix is the native conformation. During the remaining simulation times, the chain keeps the helix conformation unchanged. As a comparison, in the simulation of a free-ends chain with the same length (data not shown in this paper), the appearance of nucleation and the conformation of helix-like coil can be observed too, but there is no occurrence of helix-like cone. Clearly, this conformation is caused by the fixed end of the chain. The fixed end brings the symmetry breaking to the chain. When both ends of the chain are free to move, the chain can form and evolute to a coil from two sides equally.

In order to show the conformation evolution of the chain during simulation, we plot the contact map[19] in Fig. 3 corresponding to the diagrams in Fig. 2. To form the contact, the distance defined between a pair of non-consecutive beads is less than 6.5 Å. For the initial conformation, the contact map is empty since there is no

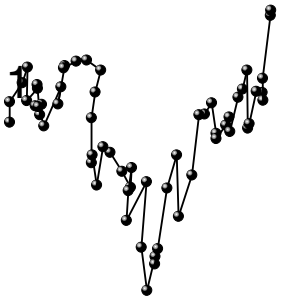

$N = 60,\ t = 1000$ h

(a)

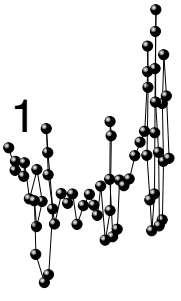

$N = 60,\ t = 10000$ h

(b)

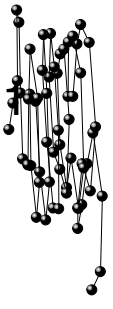

$N = 60,\ t = 23000$ h

(c)

Fig. 2. Conformations at different simulation times for chain of $N = 60$ at $T = 0.1$, the sign of "1" indicates the fixed end. (a) $t = 1000$ h, (h refers to the simulation time step), (b) $t = 10000$ h, (c) $t = 23000$ h.

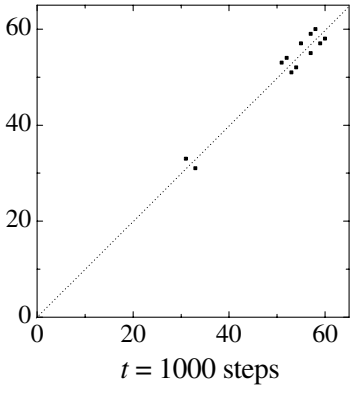

(a)

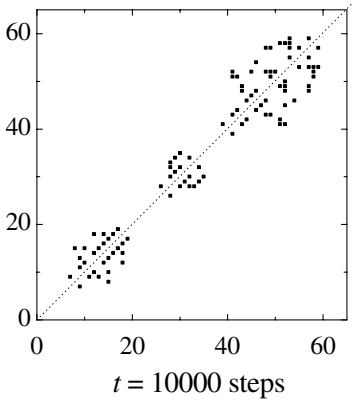

(b)

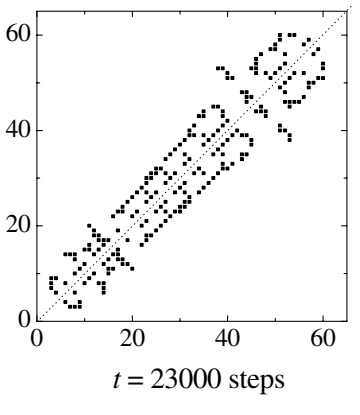

(c)

Fig. 3. Contact map for chain of $N = 60$ at $T = 0.1$. (a) $t = 1000$ h, (b) $t = 10000$ h, (c) $t = 23000$ h. These graphs show the evolution of local contacts, and hence the collapse and "folding" process.

contact at all. In Fig. 3(a), at the positions around 30th and 50th bead, there are two clusters of contacts which are parallel to the diagonal. These contacts indicate two helix-like conformations, as well as the nuclei. It is noted that if the contact is defined with $d_{ij} < 7.0$ Å, there will be an additional cluster of contacts at the position around 15th bead (figure not shown). So, there would be three helix-like coil conformations, which are also nuclei. This can be seen more clearly in Fig. 3(b). Then at the final stage there is a large helical conformation as shown in Fig. 3(c).

Figure 4 shows the fluctuations of beads under different temperatures. After reaching the equilibrium state, at low temperatures ($T = 0.1$ and 0.2), all beads have very small position fluctuations. Basically, these beads move around their equilibrium positions. However, at higher temperature ($T = 0.5$), the beads have very large position fluctuations ($\delta r_i^2 \approx 20$). The beads of $N = 15$, 23 and 55 show three minimal position fluctuations with $\delta r_i^2 \approx 14$, 12 and 10, respectively. This shows a very interesting picture for the movement of chain. These three minima relate roughly to the nuclei as mentioned above. The maximum fluctuation at the 10th bead, may be caused by the the effect of relaxing of the fixed end.

It is noted that the "folding" of short chains with $N \leq 30$ is very fast, the phenomena of coil-merging and helix-like cone are not so obvious. As shown in Fig. 5, there is only one helix-like coil in the chain at the beginning stage. Also, very quickly the helix-like coil extents to the whole chain. In other words, there are no apparent stages for coil-merging and helix-like cone, and the chain settles (or folds) to the compact state quickly and re-shapes itself to helical conformation

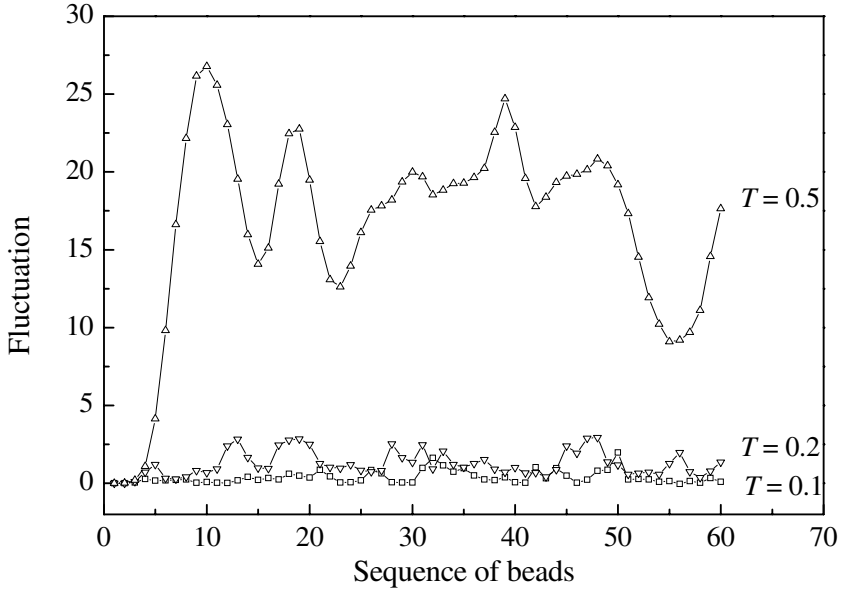

Fig. 4. Position fluctuation of each bead for chain of $N = 60$ at temperatures of $T = 0.1$, $T = 0.2$ and $T = 0.5$ after reaching the equilibrium.

easily. However, these may not indicate different "folding" mechanisms, but only a size effect. Since in the current model, each roll of helical spring at equilibrium has around 8–10 beads, then the short chains do not have enough helix-like coils to show the coil-merging and the helix-like cone, but the long chains can illustrate the whole picture well. It is also found that qualitatively, the longer the chain, the more the nuclei. The contact map for the short chain shows one cluster at the early time, and then shows a big cluster at the later time. Short chains need less time than the longer chains to form the full contact map (figures not shown).

Furthermore, we can define an equilibrium time t_e to denote the simulation steps needed to reach the equilibrium state or the "folded" state, at which the total energy and the radius of gyration do not change except for small fluctuations.

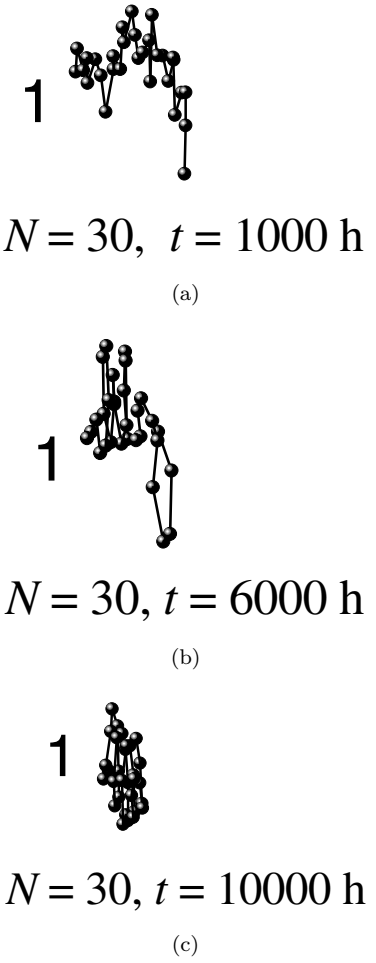

Fig. 5. Conformations at different simulation times for chain of $N = 30$ at $T = 0.1$, the sign of "1" indicates the fixed end. (a) $t = 1000$ h, (b) $t = 6000$ h, (c) $t = 10000$ h.

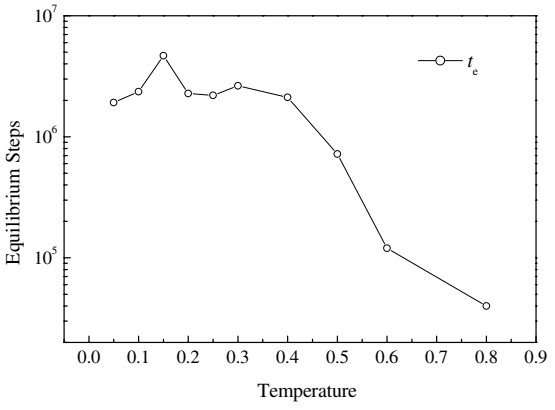

(a)

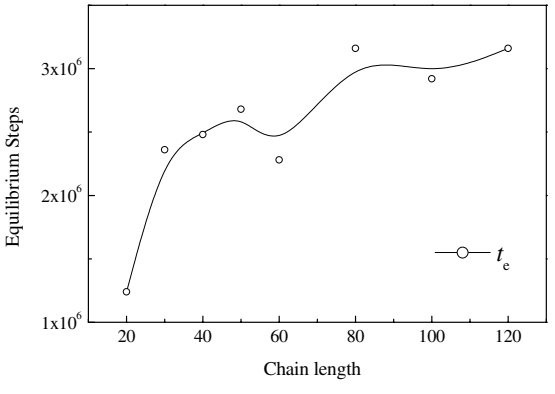

(b)

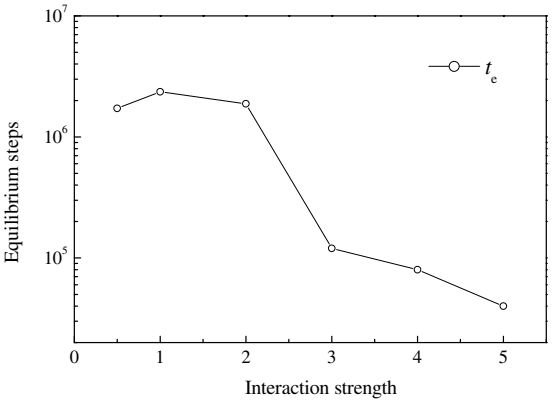

(c)

Fig. 6. The changes of equilibrium time t_e as a function of (a) simulation temperature T, while $N = 30$, $\lambda = 1.0$, (b) chain length N, while $T = 0.1$, $\lambda = 1.0$ and (c) interaction strength λ, with $N = 30$, $T = 0.1$.

The equilibrium state is a compact state, and the equilibrium time can be taken as the time at which the system firstly reaches the average equilibrated energy of that trajectory. Figure 6(a) shows t_e as a function of temperature with the chain length $N = 30$ and the interaction strength $\lambda = 1$. Generally, the higher the temperature, the smaller the t_e. In the temperature range of $T < 0.4$, in most cases, t_e is around 2×10^6, while at the high temperature range of $T > 0.6$, t_e is less than 1×10^5. The reason is at higher temperatures, the chain needs not search all the low energy states on the energy landscape and is less trapped in searching for the equilibrium state. Figure 6(b) shows the change of t_e as a function of chain length. As the chain length N increases, the value of t_e increases. When the chain length is longer than 80, the value of t_e reaches a saturated value of 3.2×10^6. This is qualitatively in accordance with the folding character of protein. The saturated value of equilibrium time can be used as the proof of avoiding the Levinthal paradox. Figure 6(c) shows the relation between t_e and λ. The equilibrium times are almost divided into two plateaus. When $\lambda \geq 3$, t_e is less than 1.2×10^5, and when $\lambda \leq 2$, t_e is around 2×10^6. This indicates that in our model, there is a critical value for interaction strength at $\lambda \approx 2.5$, above this value the chain will collapse very quickly since the interaction is very strong, and *vice versa*.

For describing the thermodynamic features of the system, we study the relation between heat capacity C_v and temperature, as well as that between radius of gyration R_g and temperature for a chain of $N = 30$. The results are shown in Fig. 7. From Fig. 7, one can see that as the temperature decreases, there are two peaks in

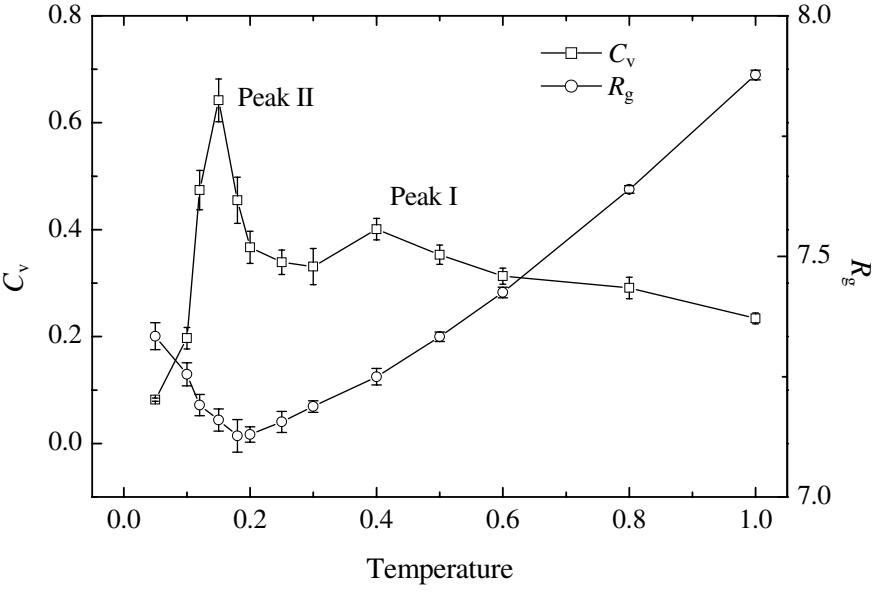

Fig. 7. Changes of heat capacity C_v and radius of gyration R_g as functions of temperature T for chain of $N = 30$.

the C_v curve at $T = 0.4$ and $T = 0.15$, but there is only one minimum in the R_g curve around $T = 0.15$. The main peak, peak-I, corresponds to the minimum of the R_g. For a typical protein, we know that as the temperature decreases, the protein chain firstly experiences a collapse transition to a compact state, then re-arranges its conformation gradually. Now in our case, although there is a collapse, the conformation is not very compact and there are large fluctuations due to the thermal effect [see Figs. 1(a) and 1(b)]. Therefore the peak-II at $T = 0.4$ is not so high. However, as the temperature decreases further to $T = 0.15$, the fluctuation becomes very small, which gives a high peak-I in the C_v curve, meanwhile a minimum value of R_g since the conformation here is very compact. From annealing simulations, it is observed that at low temperatures of $T < 0.15$, the final equilibrium conformations are helices. At higher temperatures of $0.15 < T < 0.4$, the final conformations are globular. And when $T > 0.4$, the final conformations are random-coil like. These indicate that around the temperatures of $T \approx 0.15$ and $T \approx 0.4$, there are two transitions. Clearly, peak-I relates to the so-called "folding" transition of protein, since below the temperature where peak-I sites, the chain takes the conformation of helix which is presumed as the "native" conformation due to the energy minimum. Peak-II relates to the collapse transition, and above the temperature where peak-II locates, the conformation of the chain is much looser. For a free-ends homopolymer chain with the same length, there is only one peak locating at around $T = 0.4$ with almost the same peak height, which corresponds to the collapse transition. From this meaning, fixing one end facilitates the folding and stabilizes the chain.

Now, let us present the values of T_θ, T_f, the minimal values of R_g, and the temperatures where R_g takes the minimal value as functions of chain length N and the interaction strength λ. The results are shown in Fig. 8. We can see from Fig. 8(a) that the values of T_θ and T_f change linearly with the chain length when $N < 40$. However, the relations become complicated when the chain length increases further. This is due to the increased configurational entropy effect caused by the elongated chain length. The temperature where R_g has the minimum increases monotonically with the increasing of the chain length, and so does the minimal value of the R_g. From a qualitative view, increasing the number of beads equals to increase the hydrophobic potential of the chain system, hence the temperature where R_g has the minimum, will move to higher values. In Fig. 8(b), as the interaction strength λ increases, the results are different from what in Fig. 8(a). Here, two temperatures of T_θ and T_f increase linearly as the interaction strength increases, and so does the temperature where R_g has the minimum. However, the minimal value of the R_g decreases as the interaction strength increases, but the reduction is small. These indicate that chain with stronger attractive interaction shall be more stable at higher temperatures. For example, when $\lambda = 1$, the collapse temperature is $T_\theta \approx 0.4$. Thus, at $T = 0.3$, the chain can collapse to a compact structure easily. However, if the interaction strength is reduced to $\lambda = 0.5$, the collapse temperature decreases to $T_\theta \approx 0.2$, then at $T = 0.3$ the chain no longer collapses to compact structure. Clearly, this agrees with the character of biopolymers which show less

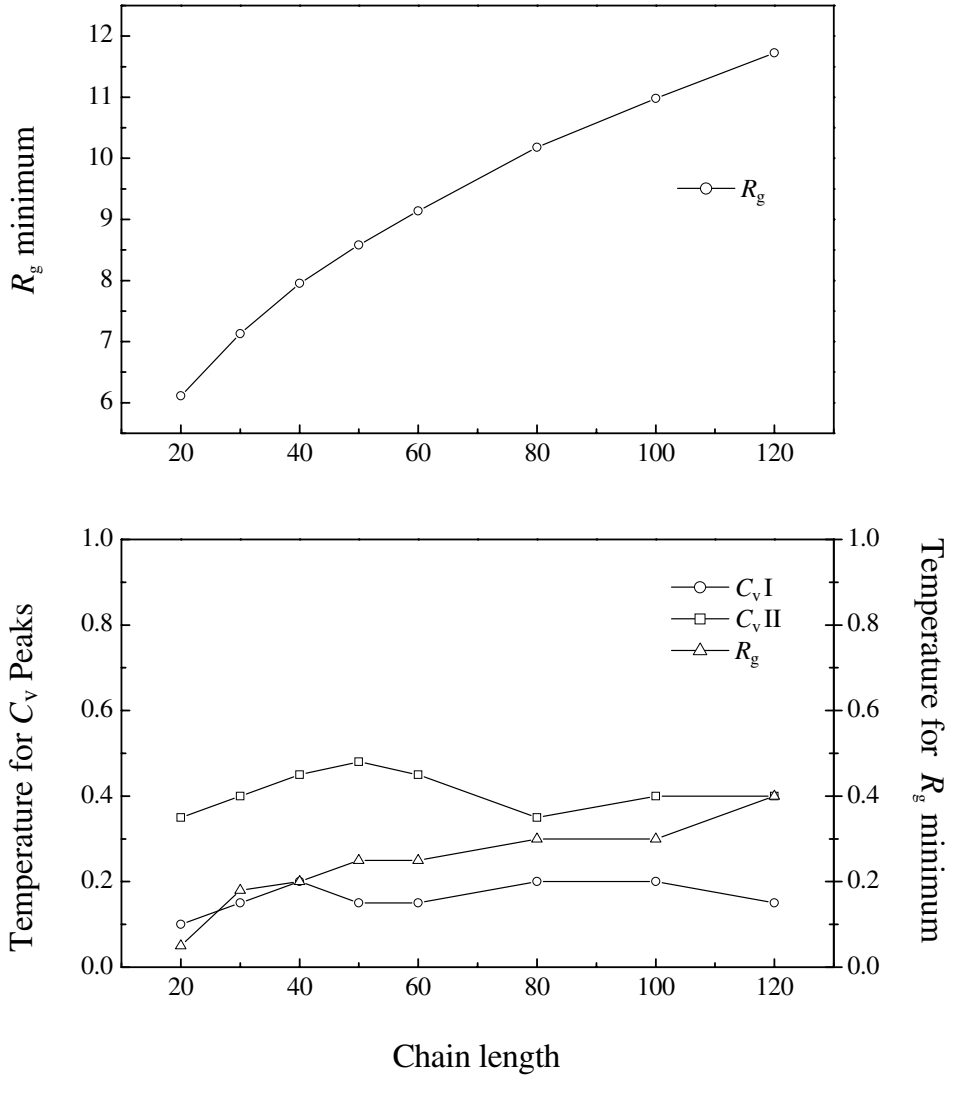

(a)

Fig. 8. For chain of $N = 30$, (a) the changes with chain length of R_g minimum, the temperature of R_g minimum and temperature of C_v peaks. C_vI and C_vII indicate the temperatures of two heat capacity peaks as shown in Fig. 7. (b) The changes with interaction strength of R_g minimum, the temperature of R_g minimum and temperature of C_v peaks.

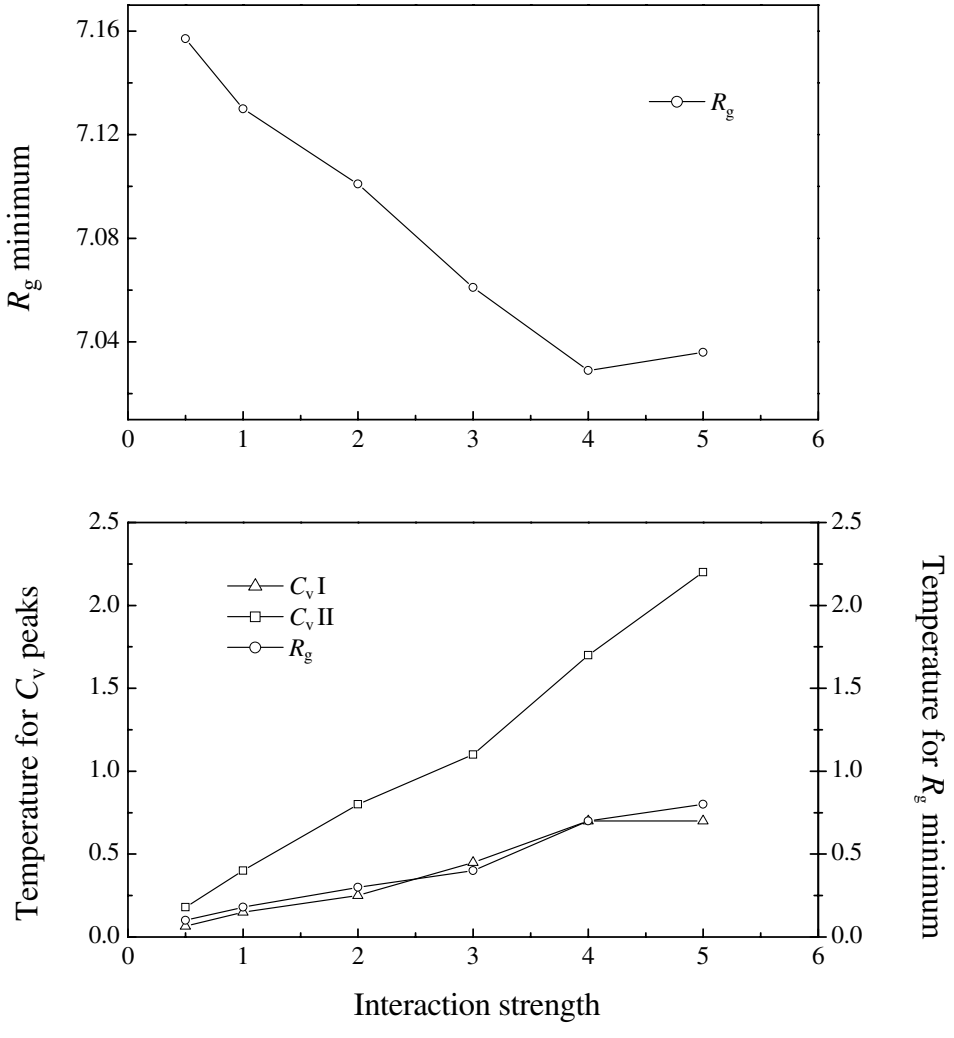

(b)

Fig. 8. (*Continued*)

stability under strong acidic or alkali circumstances. This is our qualitative interpretation. For more quantitative details, the heterogeneity shall be taken into consideration.[20] The increasing (or decreasing) of the minimal value of R_g with increasing of the chain length N (or of the interaction strength λ) is due to the strong excluded volume effect, i.e. the chain system is incompressible.

Although the chains studied in this work are homopolymer chains and they show no real folding behavior, we can still use the definition of $\sigma = (T_\theta - T_f)/T_\theta$ to see the foldability of the chains.[1] Here the temperature T_θ is the temperature where the chain experiences a conformational collapse, and T_f is the temperature where

the chain "folds" into the final equilibrium state. For the case of $N = 30$, σ is 0.625. According to the σ criterion, we can conclude that the smaller the value of σ, the better the foldability and *vice versa*. Thus the homopolymer chain is not a good folder. For better understanding of the real folding process of protein, heterogeneity shall be included.

4. Summary

We study the kinetic folding processes of homopolymers through the analysis on the conformations, the contact maps and the fluctuations of beads. We find a nuclei-regrouping process from the chains' collapse to more compact conformations for long chains ($N > 30$) with one end fixed. The chain shrinks first and creates several nuclei, then the nuclei evolve to helix-like coils starting from the free end, through the intermediate stages of coil-merging and helix-like cone. This may model a microscopic process of the adhering and adsorption of macromolecules, as well as how protein with one end fixed alters its structure. We also find that for short chains ($N < 30$), the intermediate stages do not appear obviously.

Though short and long chains do not have the same microscopic processes, their thermodynamic behaviors and macroscopic characteristics are almost the same. We find that the changes in specific heat and radius of gyration are relevant for all chain lengths. There are two peaks in the C_{v} curve, and the main peak corresponds to the minimum of R_{g}. These two quantities, namely the C_{v} and R_{g} can be combined to explain the "folding" process of the chain. Since values of T_θ and T_{f} do not change dramatically when the chain length is changed, the short and long chains have the same macroscopic "folding" features. However, the interaction strength λ affects the values of T_θ and T_{f} monotonically. Radius of gyration R_{g} increases monotonically with the chain length, but decreases monotonically with the increasing of interaction strength and there is a minimum due to the excluded volume effect. In addition, the equilibrium time gives many interesting information about the kinetics of the system.

Acknowledgments

This work was supported by the National Natural Science Foundation of China (No.90103031, 10074030, and 10021001), and the Nonlinear Project (973) of the NSM.

References

1. T. Veitshans, D. Klimov and D. Thirumalai, *Folding Des.* **2**, 1 (1997).
2. S. Takada, Z. Luthey-Schulten and P. G. Wolynes, *J. Chem. Phys.* **110**, 11616 (1999).
3. Y. Zhou, M. Karplus, J. M. Wichert and C. K. Hall, *J. Chem. Phys.* **107**, 10691 (1997).
4. T. X. Hoang and M. Cieplak, *J. Chem. Phys.* **112**, 6851 (2000).
5. A. Kolinski and J. Skolnick, *J. Chem. Phys.* **97**, 9412 (1992).

6. E. M. O'Toole and A. Z. Panagiotopoulos, *J. Chem. Phys.* **97**, 8644 (1992).
7. N. D. Socci and J. N. Onuchic, *J. Chem. Phys.* **101**, 1519 (1994).
8. E. Shakhnovich and A. Gutin, *J. Chem. Phys.* **93**, 5967 (1990).
9. U. H. E. Hansmann and Y. Okamoto, *Curr. Opin. Struc. Biol.* **9**, 177 (1999).
10. Z. W. Xing, J. Wang and W. Wang, *Phys. Rev.* **E58**, 3552 (1998); K. Fan, J. Wang and W. Wang, *ibid.* **E64**, 041907 (2001).
11. N. D. Socci and J. N. Onuchic, *J. Chem. Phys.* **103**, 4732 (1995).
12. C. J. Camacho and D. Thirumalai, *Proc. Natl. Acad. Sci.* **90**, 6369 (1993).
13. J. Wang, K. Fan and W. Wang, *Phys. Rev.* **E65**, 041925 (2002); J. Wang and W. Wang, *J. Chem. Phys.* **118**, 2952 (2003).
14. L. A. Mirny, V. Abkevich and E. Shakhnovich, *Proc. Natl. Acad. Sci.* **95**, 4976 (1998).
15. M. Compiani, P. Fariselli, P. L. Martelli and R. Casadio, *Proc. Natl. Acad. Sci.* **95**, 9290 (1998).
16. C. Clementi, A. Maritan and J. R. Banavar, *Phys. Rev. Lett.* **81**, 3287 (1998).
17. H. Noguchi and K. Yoshikawa, *J. Chem. Phys.* **113**, 854 (2000).
18. H. J. C. Berendsen, J. P. M. Postma, W. F. van Gunstern, A. Dinola and J. R. Haak, *J. Comput. Phys.* **81**, 3684 (1984).
19. H. S. Chan and K. A. Dill, *J. Chem. Phys.* **92**, 3118 (1990).
20. U. H. E. Hansmann, M. Masuya and Y. Okamoto, *Proc. Natl. Acad. Sci.* **94**, 10652 (1997).